J. Phys.: Condens. Matter 1 4387 (1989)

Rb_2CrCl_4: Studies of a Two Dimensional Classical Easy-Plane Heisenberg Model with in-plane Symmetry Breaking

M. E. Gouvea*, G. M. Wysin, A. R. Bishop
Los Alamos National Laboratory
Los Alamos, NM 87545 USA

and

F. G. Mertens
Physics Institute, University of Bayreuth
D-8580 Bayreuth, Fed. Rep. of Germany

ABSTRACT

We present numerical simulation studies on the two-dimensional easy-plane classical ferromagnetic Heisenberg model with 4-fold in-plane symmetry breaking. Continuum limit equations of motion are obtained and some nonlinear particular solutions are discussed. Our simulation data are compared with experimental data obtained for Rb_2CrCl_4. We find evidence for two transition temperatures in this model.

*Supported by CNPq (Conselho Nacional para o Desenvolvimento Cientifico e Tecnologico, Brazil) and by UFMG (Universidade Federal de Minas Gerais).

INTRODUCTION

In recent years there has been a considerable amount of theoretical work [Regnault and Rossad-Mignod, 198~~6~~7] concentrated on two-dimensional (2D) or quasi-2D physical systems. Magnetic 2D-systems are particularly interesting since they allow treatment based on simple model spin-Hamiltonians which have successfully described linear spin-waves. Several possibilities of ferro- and antiferromagnetic isotropic or anisotropic exchange interactions and, also, in-plane symmetry breaking can be analytically or numerically studied. Depending on the particular features of each model there can be, for example, one or more 'phase transitions.' In a classical picture, nonlinear domain-walls, vortices and spin-waves are potentially important elementary excitations for the understanding of these models. For a system with easy-plane symmetry there is a topological transition associated with the unbinding of vortex-antivortex pairs [Kosterlitz and Thouless, 1973] and an additional in-plane symmetry breaking can lead to a further transition depending on the degree of symmetry breaking [Jose et al., 1977].

Improvements in materials preparation have made available a considerable number of materials that can be classified as quasi 2D-magnets. The primary characteristic of such materials is that the interplanar interaction is much smaller than the intraplanar one so that they behave predominantly two dimensionally, even in the vicinity of T_c if the 3D fluctuations are still weak enough to be outside the 3D critical regime[Regnault et al., 1987].

Rubidium chromous chloride (Rb_2CrCl_4) is one of these layered-type magnets; the nearest neighbor (n.n.) interplanar interaction is $\sim 10^{-4}$ the n.n. intraplanar interaction [Hutchings et al., 1981]. This weak interplanar coupling is responsible for a 3D-ordering at T_c=52.2K. Several experimental works [Fair et al, 1978; Lindgard et al., 1980; Hutchings et al., 1981, 1986; Cornelius et al., 1986; Kleemann et al., 1986] have studied the properties of this compound and, by now, it is well established that the dominant interaction is a ferromagnetic exchange between the n.n. <u>in</u> the planes, and that single ion terms restrict the spins' movement to these planes (i.e., easy plane anisotropy). In terms of these properties Rb_2CrCl_4 is somewhat similar to K_2CuF_4, another quasi-2D magnetic material which has been extensively studied [Funahashi et al., 1976; Moussa and Villain, 1977; and Hirakawa et al., 1981, 1982]. There are, however, important differences between these two compounds. The Cu^{2+} ion in K_2CuF_4 has S= 1/2 and no in-plane anisotropy is expected in the Hamiltonian. The Cr^{2+} in Rb_2CrCl_4 has a larger spin, S=2, and is thus expected to behave more classically; moreover it is subject to single-ion anisotropy effects which tend to align spins along the [110] and symmetry related directions. Although K_2CuF_4 cannot be classified as a true 2D-XY magnet, because the interaction is dominantly of Heisenberg type, magnetic measurements and neutron scattering studies have suggested that the transition has a Kosterlitz-Thousless (KT) character, reflecting some easy-plane anisotropy. Observed critical parameters including the inverse correlation length, k, and the critical exponent η can be fitted to KT theory with reasonable success. The experimental results are consistent with vortex theory [Hikami and Tsuneto, 1980] and with Monte Carlo (MC) simulations [Kawabata and Bishop, 1986a] which have shown that the transition temperature T_{KT} is weakly dependent on the easy-plane anisotropy, except when very close to the Heisenberg model (those works have not considered an in-plane anisotropy). Similar attempts to identify a KT-transition have been made in Rb_2CrCl_4 but a definite conclusion has not been achieved and it is interesting to understand to what extent the in-plane anisotropy is responsible for the observed discrepancies.

At this point, it is useful to give a brief summary of some of the experimental results obtained for Rb_2CrCl_4. Inelastic neutron scattering techniques have been used to investigate the low wavevector spin waves at several temperatures below T_c. Sharp spin waves are observed at all q [Hutchings et al., 1981, 1986 and references cited therein] with a gap at q=0 due to the in-plane anisotropy. The low wave vector spin waves renormalize anomalously as the temperature increases towards T_c. Similar renormalization effects were observed in K_2CuF_4 and have been attributed to 2D-XY behavior [Hirakawa et al, 1983] which leads to a universal jump in the stiffness constant at T_{KT} [Nelson and Kosterlitz, 1979]. However, concerning Rb_2CrCl_4, it is not yet clear what is the cause of this anomalous renormalization. Extensive magnetisation studies [Cornelius et al., 1986] reveal that an isothermal critical behavior as $M \alpha H^{1/\delta}$ (M is the magnetisation and H is the applied field), at low temperatures, leads to a temperature dependence for the δ exponent; another characteristic behavior predicted by KT-theory. Associating T_{KT} with the temperature at which $\delta = 15$ [Kosterlitz, 1974], the value $T_{KT} = 45.5K$ was obtained. However, above T_c the susceptibility can be fitted equally well to a KT-theory or to a conventional power-law behavior and, as said before, the final results do not permit us to unambiguously identify the true nature of the critical behavior of Rb_2CrCl_4.

Our aim in this work is to provide some additional information on dynamics for this particular class of easy-plane ferromagnets with in-plane symmetry breaking. Some MC studies for 2D-easy plane Heisenberg models with Ising and 6-fold in-plane symmetry breaking have been performed by Kawabata and Bishop (1986 b) but only static thermodynamic properties were studied. Based on a simplified model Hamiltonian proposed by Hutchings et al. (1981), those authors considered the Ising in-plane symmetry breaking as appropriate for describing Rb_2CrCl_4. We will discuss the relevance of considering the full Hamiltonian (Section II) A four-fold symmetry breaking (denoted by $p = 4$), as appropriate to Rb_2CrCl_4, is particularly interesting since we know from the work of Jose et al. [1977] that $p = 4$ corresponds to a kind of "border-line" in the sense that system with $p < 4$ are <u>not</u> expected to show a KT-transition while systems with $p > 4$ are expected to show two transitions, one of which can be related to a KT-transition, and the other to domain ordering. However, those theoretical results were obtained for the planar-model and could be modified when out-of-plane spin components are included. Here we have investigated the $p = 4$ case with numerical simulations using a combined Monte Carlo-Molecular Dynamics (MC-MD) approach. A (microcanonical) MD integration of equations of motion was performed using initial configurations generated by a MC simulation. The total space-time Fourier transform of the correlation function $S(q,\omega)$ includes the effect of all excitations and their interactions. Since there are no 3D-effects, we have the advantage of isolating purely 2D information. Unfortunately, at this time there is no available theory which includes domain-walls, vortices, spin-waves and interactions between them to which we can compare our numerical experiments. We believe that all these excitations must be considered in order to understand the dynamical aspects related to this system. Nevertheless, the analysis of our simulation data provides useful information, including the existence of two transition temperatures for Rb_2CrCl_4.

The paper is organized as follows: in Section II, we discuss the model Hamiltonian to be used in our studies of Rb_2CrCl_4 including improvements to previous models so as to accommodate large amplitude (nonlinear) excitations; Section III contains the equations of motion obtained in the context of a continuum theory. Some particular solutions to these equations are also discussed. We present our simulation data and analysis in Section IV and the final conclusions are given in Section V.

II. MODEL HAMILTONIAN FOR Rb_2CrCl_4

It has been established that the magnetic ions in Rb_2CrCl_4 lie in planar square arrays and are coupled via Cl-ions situated between them but displaced from the middle of the Cr^{2+}-positions [Le Dang et al., 1977; Day et al., 1979]. This distortion causes alternate atoms to have an easy axis in the x and y direction, respectively. The previously proposed spin Hamiltonian is

$$H = -J\sum_{ij} \vec{S}_i \cdot \vec{S}_j - G\sum_{i} \left[\left(S^x_{i1}\right)^2 + \left(S^y_{i2}\right)^2\right] + D\sum_{i} \left(S^z_i\right)^2, \qquad \text{(II.1)}$$

The parameters involved have been measured from linear spin-wave dispersion data [Hutchings et al., 1981]. J = 15.12K is the nearest neighbor ferromagnetic exchange constant, $G = 3.14K$ is the staggered single-ion anisotropy constant creating two sublattices, 1 and 2, and $D = -0.14K$ is the planar anisotropy constant. Despite the negative value of D, we still have planar-behavior assured by the high value taken by G.

It has been found [Hutchings et al., 1981] that the linear spin-wave dispersion of Rb_2CrCl_4 is also well described by the following simple model Hamiltonian

$$\tilde{H} = -\tilde{J}\sum_{ij} \vec{S}_i \vec{S}_j + \tilde{D}\sum_i \left(S_i^z\right)^2 - \tilde{G}\sum_i \left(S_i^d\right)^2 \tag{II.2}$$

where d is along [110] and

$$\tilde{J} = J \cos 2\alpha; \tilde{G} = G \sin 2\alpha; \tilde{D} = D + (P/2)\,[1 - \sin 2\alpha] \tag{II.3}$$

$\alpha = G/8J$ corresponds to the canting angle and can be determined by minimizing the classical internal energy. Hamiltonian (II.2) is an approximation to (II.1) obtained through a rotation around the z-axis and by neglecting the canted two-sublattice structure.

It is important to emphasize that Hamiltonians (II.1) and (II.2) correspond to different in-plane symmetry breaking which becomes important for non-linear effects; we have a four-fold in-plane symmetry from equation (II.1) while equation (II.2) describes a two-fold or Ising-like symmetry. It is not surprising that linear spin-wave dispersion data can be described equally well by both Hamiltonians since the spin wave dispersion is independent of the degree of symmetry breaking. (That is, spin waves are perturbations from one of the ground state configurations). Nevertheless, as was briefly discussed in Section I, the degree of the in-plane symmetry can be decisive in determining whether a KT-transition is possible in these easy-plane magnets. We can expect that each of these two Hamiltonians supports different nonlinear dynamical features. We can note that simply rotating the xy coordinate system by 45°, and retaining the two sublattice model leads to a Hamiltonian exactly equivalent to (II.1),

$$H = -\tilde{J}\sum_{ij} \vec{S}_i \cdot \vec{S}_j + (\tilde{D} + 1/2\,\tilde{G})\sum_i \left(S_i^z\right)^2 - \tilde{G}\sum_i S_{i1}^{x'} S_{i1}^{y'} + \tilde{G}\sum_i S_{i2}^{x'} S_{i2}^{y'} \,.$$

The primes indicate the new coordinate system where x' is along [110]. The competition between the strong n.n. exchange and the sublattice-dependent two-fold in-plane anisotropies (note that they are oriented at 90° to each other) results in an effective four-fold symmetry, plus a small canting. For an accurate description of large amplitude nonlinear excitations in Rb_2CrCl_4, such as domain walls, it is essential that we use a model Hamiltonian with the correct ($p = 4$) symmetry. In particular, for domain walls, a $p = 4$ Hamiltonian will support 90° domain walls connecting the degenerate in-plane ground states, and a description by a $p = 2$ Hamiltonian can include only 180° domain walls. Also, the interactions of in-plane vortices with these domain walls will be dependent on the total "twist" of the walls. Since T_{KT} can be expected to be a sizable fraction of JS^2, it is likely that domain walls may be easily created near the transition temperature and therefore they can play a part in modifying the transition through their interactions with vortices. As a result of this, we expect that an accurate description of a possible symmetry-modified KT-transition in Rb_2CrCl_4 will require a model which correctly describes the domain walls and their effect on the vortices (and vice-versa). For this reason, we have used Hamiltonian (II.1) in our MC-MD simulation studies for Rb_2CrCl_4.

III. CONTINUUM THEORY FOR Rb_2CrCl_4

The spin components can be described by four angular variables since we have two sublattices. Adopting a procedure similar to the one used by Mikeska (1980) for the antiferromagnetic chain we define

$$S_{n,m} = S \begin{array}{l} \cos[\Theta_{n,m} + (-1)^{n+m}\theta_{n,m}]\cos[\Phi_{n,m} + (-1)^{n+m}\phi_{n,m}];\ \cos[\Theta_{n,m} \\ + (-1)^{n+m}\theta_{n,m}] \times \sin[\Phi_{n,m} + (-1)^{n+m}\phi_{n,m}];\sin[\Theta_{n,m} + (-1)^{n+m}\theta_{n,m}] \end{array} . \quad \text{(III.1)}$$

where (n, m) denotes the spin site in the 2D-lattice. For the continuum classical dynamics, we assume that the spin-fields $\Theta(\mathbf{r})$, $\Phi(\mathbf{r})$, $\theta(\mathbf{r})$ and $\phi(\mathbf{r})$ [$\mathbf{r} = (r, p)$ in polar coordinates] vary smoothly and also that $\theta(\mathbf{r}), \phi(\mathbf{r})$ represent small deviations from $\Theta(\mathbf{r})$ and $\Phi(\mathbf{r})$, respectively. Including terms up to second order in spatial derivatives, the continuum equations of motion are

$$\frac{1}{JS}\Theta = -8\,\phi\,\theta\,\sin\Theta - 2\sin\Theta\,\nabla\Theta\cdot\nabla\Phi + \cos^2\Phi\,\nabla^2\Phi + g\,\theta\sin\Theta\sin 2\Phi - 2g\,\phi\cos\Theta\cos 2\Phi \qquad \text{(III.2)}$$

$$\frac{1}{JS}\Phi = \frac{8\theta^2\sin\Theta}{\cos^2\Theta} - 8\phi^2\sin\Theta - \sin\Theta\left(\nabla\Phi\right)^2 - \frac{\nabla^2\Theta}{\cos\Theta} + 2d\sin\Theta + g\sin\Theta\,[1 - 2\phi\sin 2\Phi + g\theta\cos\Theta\cos 2\Phi \qquad \text{(III.3)}$$

$$\frac{1}{JS}\theta = -8\,\phi\cos\Theta - g\cos\Theta\sin 2\Phi \qquad \text{(III.4)}$$

$$\frac{1}{JS}\phi = \frac{8\theta}{\cos\Theta} + 2d\cos\Theta + g\,\theta\cos\Theta + g\sin\Theta\cos 2\Phi\,, \qquad \text{(III.5)}$$

where $g = G/J$ and $d = D/J$.

It is hard to obtain general solutions to equations (III.2-5)., We will limit ourselves here to some particular cases. One obvious particular static solution $(\Theta = \Phi = \phi = \theta = 0)$ corresponds to

$$\Theta = \theta = 0\ ;\ \Phi = \pm\frac{\pi}{4} \qquad \text{(III.6a)}$$

$$\phi = \frac{g}{8}\sin 2\Phi \qquad \text{(III.6b)}$$

.i.e., planar domains oriented along the [±,1,±1,0] directions. Equation (III.6b) gives the canted structure. Another planar ($\Theta = \theta = 0$) static solution is given by

$$\nabla^2\Phi = \frac{-g^2}{8}\sin 4\,\Phi \tag{III.7}$$

and Equation (III.6b) for ϕ. Equation (III.7) is a sine-Gordon equation for the Φ variable and the argument of the sine function (4Φ) reflects the 4-fold in-plane symmetry breaking. This equation has been studied by Hudak (1982) who obtained a vortex-like solution

$$\phi = \pm\tan^{-1}\left\{\left[\sinh\left(g\frac{(y-y_0)}{2}\right]\left[\sinh\left(\frac{g(x-x_0)}{2}\right)\right]^{-1}\right\} + (2n+1)\frac{\pi}{2} \tag{III.8}$$

(where n is an integer number) with vorticity ± 1 and which is shown in fig. [1]. It can be seen that in the region surrounding the vortex center (x_0, y_0) the vortex described by (III.8) does not appreciably differ from the usual vortex $\Phi = \pm\tan^{-1}$ (y/x) of the planar model. The difference, however, is strong in the far-field region where the spins form four domains separated from each other by domain walls along $\Phi = (2n+1)\pi/4$ (n = 0,+1,...). The energy of this vortex was also estimated by Hudak (1982) and depends linearly on L, the system size. Recall that the energy of a single planar-model vortex diverges logarithmically with the size of the system. This logarithmic dependence comes from the fact that, for the planar-model, the required 2π–rotation of a vortex can be approximately equally divided among all nearest neighbor pairs and as we transverse a circle of radius r having the vortex at its center, the spins are rotated from their neighbors by an angle ~1/r (Einhorn et al., 1980). The in-plane symmetry of our model does not permit the spins to equally share the 2π–rotation and they change their orientation by $\pi/2$ when crossing the domain boundaries. Since the domain boundaries have finite energy per unit length, the energy for a single vortex diverges with L, as found by Hudak, and we should not expect to find vortices, at least at low temperatures. However, vortex-antivortex pairs bound by domain boundaries (strings) have finite energy and can be created giving rise to a linear interaction potential between vortices.

Entropy arguments [Lee and Grinstein, 1985, Einhorn et al., 1980, Tang and Mahanti, 1986] can be used to determine the phase diagram. Generally speaking, we could expect a transition temperature T_1 such that at $T>T_1$ the strings connecting vortex-antivortex pairs become flexible, and a transition temperature $T_2=T_{KT}$ due to the unbinding of these pairs. The phase diagram is determined by the relative magnitudes of T_1 and T_2. Our simulation studies (Section IV) for Hamiltonian (II.1) suggest two transition temperatures, i.e., $T_1<T_2$.

The particular solutions we have discussed here are restricted to the XY plane. It is interesting to ask whether Equations (III.2) to (III.5) also admit static vortex-like solutions with non-zero out-of-plane spin components in the region close to the vortex-center. This kind of solution has been found by Hikami and Tsuneto (1980) for the anisotropic Heisenberg model (without single ion anisotropy terms). It has been found that the stability of this vortex-like solution depends on the easy-plane anisotropy [Wysin et al., 1988]. The vortex shape is crucial in determining the out-of-plane correlation function, as discussed in a phenomenological model by Mertens et al. (1987, 1988).

IV. NUMERICAL SIMULATION AND ANALYSIS

A Combined MC-MD method [Kawabata et al. (1986)] was used to determine the equilibrium dynamics, especially for the dynamic structure function $S(\vec{q},\omega)$. Simulations were performed on a 100x100 square lattice for model (II.1), with periodic boundary conditions. In this method, first a MC simulation is performed, producing a set of equilibrium configurations for a desired temperature. These configurations are then used as initial conditions for an energy-conserving MD simulation of the equations of motion. The time integration was performed with a standard fourth order Runge-Kutta method, with a fixed time step of 0.04 $(JS)^{-1}$. The spin configuration was sampled at 512 equally spaced times, so that an FFT algorithm could be used for the temporal part of the space-time Fourier transform. To adequately resolve spin wave peaks for the smallest wavevectors $(q=(1/100)2\pi/a)$, it was necessary to integrate to $t\approx654$ $(JS)^{-1}$. The dynamic structure function $S^{\alpha\alpha}(\vec{q}, \omega)$ was then determined from the Fourier transform of the space-and time-displaced correlation function, $<S^{\alpha}(\vec{0}, 0)S^{\alpha}(\vec{r}, t)>$. In particular we calculated in-plane correlations (α=x,y) and out-of-plane correlations (α=z). The structure functions resulting from several initial conditions for a given temperature were then averaged together. Typically, we averaged over only three initial conditions, because the calculations required about 30 cpu minutes per initial condition on a CRAY-1S vector machine. We also employed a smoothing algorithm on $S(\vec{q},\omega)$, as in Mertens et al. (1987, 1988), to reduce the effects of a finite time series and statistical fluctuations.

Figures 2(a,b,c) show spin orientation-plots taken at several temperatures. From the spin orientations at the lowest temperature, $T=0.4JS^2$, it can be seen that the spins are largely confined to the XY plane. It is possible to identify small domains with the spin polarization rotated by $\pi/2$ with respect to other domains. As the temperature increases, the out-of-plane spin components increase and, although the plots become increasingly difficult to analyze, we can see that the domain's size decrease, consistent with entropy arguments [Einhorn et al, 1980]. For $T=0.7JS^2$ and $T=0.9JS^2$, figures 2(b) and 2(c), we can identify vortex-like structures and we notice that they have appreciable out-of-plane spin components close to the vortex-center.

The space time Fourier transforms of the correlation functions $S_{xx}(q,\omega)$ and $S_{zz}(q,\omega)$, for $q=(q,0)$, are shown in figures 3(a, b). A <u>central-peak</u> can be seen for all temperatures considered in both in-plane and out-of-plane correlation functions, althought it is more intense for $S_{xx}(q,\omega)$ than for $S_{zz}(q,\omega)$ at low temperatures. Experimentally, a central peak has been observed [Hutchings et al, 1986] near $T_c\approx0.86JS^2$, the temperature at which 3D-ordering occurs. The width Γ_x is seen to vary approximately linearly with q for $T<T_c$ and quadratically for $T>T_c$. This central peak was fitted to a product of two Lorentzians, one for the ω-dependence and one for the q-dependence. Such a Lorentzian in-plane central peak has been proposed on the basis of a phenomenological theory [Mertens et al., 1987, 1988] for the anisotropic Heisenberg model as due to a "gas" of unbound vortices. The experimental data also give a non-null Γ_x at $q = 0$ (at $T = T_c > T_{KT}$) as predicted by that phenomenology. The q-dependence of Γ_x for $T = 0.8JS^2$ and $T = 0.9JS^2$, as extracted from our simulation data, is shown in figures 4 (a,b). It is clear that Γ_x shows distinct behavior for $q<q_C$ ($q_C \alpha \xi^{-1}$ where ξ is the correlation length), which is also in agreement with the phenomenological theory: for $q<q_C$, Γ_x varies smoothly with q while for $q>q_C$ we have, roughly $\Gamma_x \alpha q^2$ (for the XY model, the phenomenology predicts Γ_x varying as $\Gamma\alpha$ (constant $+q^2$) for small q ($q<<\xi^{-1}$) and as $\Gamma_x \alpha q$ for $q>>\xi^{-1}$). We emphasize that this phenomenological theory does not include an in-plane anisotropy and discrepancies when comparing it to our system can be expected. However the qualitative agreement mentioned above suggests that scattering within a gas of vortices can be the dominant contribution to the central peak for temperatures above T_{KT}. For temperatures below T_{KT}, where the vortices are bound into pairs, another mechanism is required for the central peak and domain walls fluctuations are good candidates. Unfortunately, at the present time, assumptions like these cannot be checked because of the lack of an adequate dynamical theory.

The spin wave spectrum has been evaluated to first order in the Holstein-Primakoff approximation by Elliott et al., (1980)

$$\omega_q = 2JS\left[2\cos 2\alpha + g\sin 2\alpha - \cos 2\alpha\,(\cos q_x + \cos q_x\right]^{1/2} \times \left[2\cos 2\alpha + d + \frac{g}{2}(1+\sin 2\alpha) - (\cos q_x + \cos q_x)\right]^{1/2} \tag{IV.1}$$

For finite T, the spectrum has been calculated by Lindgard et al. (1980) who also included zero-point quantum corrections. Figures 5(a, b) show the spin-wave dispersion obtained from our simulation data for wave vectors along $[\zeta,0,0]$ and $[\zeta,\zeta,0]$ directions at $T=0.5JS^2$. The continuous curve corresponds to eq. (IV.1). It can be seen that the relative renormalization of the mode in the $[\zeta,0,0]$ direction is less pronounced than that of the $[\zeta,\zeta,0]$ mode. A similar observation was made by Fair et al., (1978) for [0.15,0,0] and [0.1, 0.1, 0] modes which have only slightly different wave vectors and energies. This effect can be due to the in-plane four-fold symmetry. In figure (6) we show how the low wave vector spin-waves renormalize as the temperature increases. As pointed out in Section I, an anomalous renormalization has been experimentally observed [Hutchings et al., 1981] and is strongly wave vector dependent, being greatest for the low wave vector modes. This wave vector dependence is also shown in figure (6).

Figures 7 (a,b) show the product of the height of the central peak, $S_{\alpha\alpha}(q,\omega=0)$ $[\alpha=x,z]$ and the width $\Gamma_{\alpha}(q)$ as a function of T for low wave vectors. This product is proportional to the intensity of the central peak (the proportionality constant depends on the shape of the peak) which, in the limit $q\rightarrow 0$, can be related to the magnetic susceptibility. These graphs suggest two transition temperatures around $T_1 \equiv 0.5JS^2 \equiv$ and $T_2 \equiv 0.8JS^2$: we recall that $T=0.75JS^2$ has been identified as a possible value for T_{KT}. Simulation studies performed by Kawabata and Bishop (1986) using the simplified Hamiltonian, eq. (II.2), also give evidence for two transition temperatures ($T_1 \equiv 0.3JS^2, T_2 \equiv 0.8JS^2$).

V. Conclusion

In this work, we have discussed the effects of in-plane anisotropy fields on the large amplitude nonlinear excitations of 2D-easy plane Heisenberg models. In particular, for Rb_2CrCl_4 we emphasize the relevance of taking the full Hamiltonian given by equation (II.1) in order to properly describe domain walls and their interaction with vortices.

The comparison between our simulation and experimental data show good qualitative agreement. We were able to observe the spin-wave renormalization as the temperature increases for both ω_{xx} and ω_{zz} [figures (6a, b)] where ω_{xx} and ω_{zz} are spin wave frequencies determined from the in-plane correlation, $S_{xx}(q, \omega)$, and out-of-plane correlation, S_{zz} (q, ω), respectively. The experimental results, taken from neutron scattering experiments, correspond to ω_{xx} renormalization. Recent simulation studies (Wysin et al., 1988) on the 2D-XY ferromagnetic model also show that both ω_{xx} and ω_{zz} renormalize when $T \rightarrow T_{KT}$, but the softening of ω_{xx} is much stronger than for ω_{zz}. Here the softenings of ω_{zz} and ω_{xx} are comparable and this can be due to the fact that the interaction is predominantly of the Heisenberg type. On the other hand, the in-plane anisotropy seems to be responsible for the differences observed in the spin-wave dispersion for wavevectors along the [ζ,0,0] and [ζ,ζ,0] directions.

The simulation data also present evidence for two transition temperatures around $T_1 \cong 0.5JS^2$ and $T_2 \cong 0.8JS^2$. Experimentally, it would be very difficult to observe the lower transition, T_1, because it is well below the 3D-ordering temperature, but the value found for T_2 is in good agreement with the value $T \cong 0.75JS^2$ which has been identified previously as a possible value for T_{KT} for Rb_2CrCl_4.

REFERENCES

Cornelius C. A., Day P., Fyne P. J., Hutchings M. T. and Walker P. J., 1986 J. Phys. C19, 909

Day P., Hutchings M. T., Janke E. and Walker P. J., 1979 J. Chem. Soc. Chem. Commun. 711

Einhorn M. B., Savit R. and Ravinovici E. 1980 Nuclear Phys. B 170, 16

Elliott R. J., Hengeltraub A., Harrop M. C. and Ziman T. A. L., 1980 J. Magn. Magn. Mat. 15-18, 359

Fair M. J., Hutchings M. T., Day P., Ghosh R. and Walker P. J., 1978 J. Phys. C 11, L813

Funahashi A., Moussa F. and Steiner M., 1976 Sol. State Commun. 18, 433

Hikami S. and Tsuneto T., 1980 Prog. Theor. Phys. 63, 387

Hikakawa S. and Ubukoschi K., 1981 Phys. Soc. Jpn. 50, 1909

Hikakawa K., Yoshizawa H. and Ubukoschi K., 1982 J. Phys. Soc. Jpn. 51, 2151

Hikakawa K., Yoshizawa H., Axe J. D. and Shirane G. 1983 J. Phys. Soc. Jpn. 52, 4220

Hudak O., 1982 Phys. Lett. 89A, 245

Hutchings M. T., Als-Nielsen J., Lindgard P. A. and Walker P. J., 1981 J. Phys. C 14, 5327

Hutchings M. T., Day P., Janke E. and Pynn R., 1986 J. Magn. Magn. Mat. 54-57, 673

Jose J. V., Kadanoff L. P., Kirkpatrick S. and Nelson D. R. 1977 Phys. Rev. B 16, 1217

Kawabata C. and Bishop A. R., 1986a Sol. State Commun. 60, 169

Kawabata C. and Bishop A. R., 1986 b Z Phys. B 65, 225

Kawabata C., Takeuchi M., Bishop A. R. 1986 J. Magn. Magn. Mat. 54-57, 871

Kleeman W., Otte D., Usadel K. D. and Brieskorn G., 1986 J. Phys. C 19 395

Kosterlitz J. M. and Thouless D. J., 1973 J. Phys. C 6, 1181

Kosterlitz J. M., 1974 J. Phys. C 7, 146

De Lang K., Veillet P. and P. Walker, 1977 J. Phys. C 10, 4593

Lee D. H. and Grinstein G. 1985 Phys. Rev. Lett. 55, 541

Lindgard P. A., Als-Nielsen J. and Hutchings M. T., 1980 J. Magn. Magn. Mat. 15-18, 343

Mertens, F. G., Bishop A. R., Wysin G. M., and Kawabata C., 1987 Phys. Rev. Lett. 59, 117

Mertens, F. G., Bishop A. R., Wysin G. M. and Kawabata C., 1988 Phys. Rev. B - in press

Mikeska H. J., 1980 J. Phys. C 13, 2913

Moussa F. and Villain J., 1977 Physica B 86-88, 696

Regnault L. P. and Rossad-Mignod J. 1987 in "Magnetic Properties of Layered Transition Metal Compounds," -eds. L. J. Jongh and R. D. Willet (Reidel, Dordricht)

Tang S. and Mahanti S. D., 1986 Phys. Rev. B 33, 3419

Wysin G., Gouvea M. E., Bishop A. R., Mertens F. G. (1988) in: "Computer Simulation Studies in Condensed Matter Physics: Recent Developments" (Springer, Berlin), in press

FIGURE CAPTIONS

Figure 1. A single vortex given by eq. (III.8) [with $x_0=y_0=0$, n=g=1] plotted on a square lattice.

Figure 2. Spin (orientation plots taken at a) $T=0.4JS^2$, b $T=0.7JS^2$ and c) $T=0.9JS^2$ from our numerical simulation. The lengths of the lines are proportional to the in-plane spin components. Black and white arrows indicate, respectively, positive and negative out-of-plane spin components.

Figure 3. Results from MC-MD simulations of Hamiltonian (II.1) on a 100 x 100 lattice for $\vec{q}=(0.10,0)$ π/a for a) in-plane correlations and b) out-of-plane correlations. Data taken at two temperatures are shown; $T=0.5JS^2$ and $T=0.8JS^2$.

Figure 4. Width Γ_x of central peak in S_{xx} $\overrightarrow{(q,\omega)}$ for a) $T=0.8JS^2$ and b) $T=0.9JS^2$. Data points and error bars rresults from estimating Γ_x from plots like Figure 3.

Figure 5. Spin-wave dispersion obtained from the simulation data for wavevectors along a) $[\zeta,0]$ and b) $[\zeta\zeta]$ directions at $T = 0.5JS^2$ The crosses and circles correspond, respectively, to data taken from S_{zz} (q,ω) and $S_{xx}(q,\omega)$ curves. The continuous curve corresponds to eq. (IV.1).

Figure 6. Spin-wave frequencies (from our simulations) as functions of temperature determined from a) in-plane correlations, Sxx (q,ω), and b) out-of-plane correlations, S_{zz} (q,ω).

Figure 7. Height of the central peak, $S_{\alpha\alpha}(q,\omega=0)$ [a) $\alpha=x$ and b) $\alpha=z$)] times the width Γ_α (q) as a function of T.

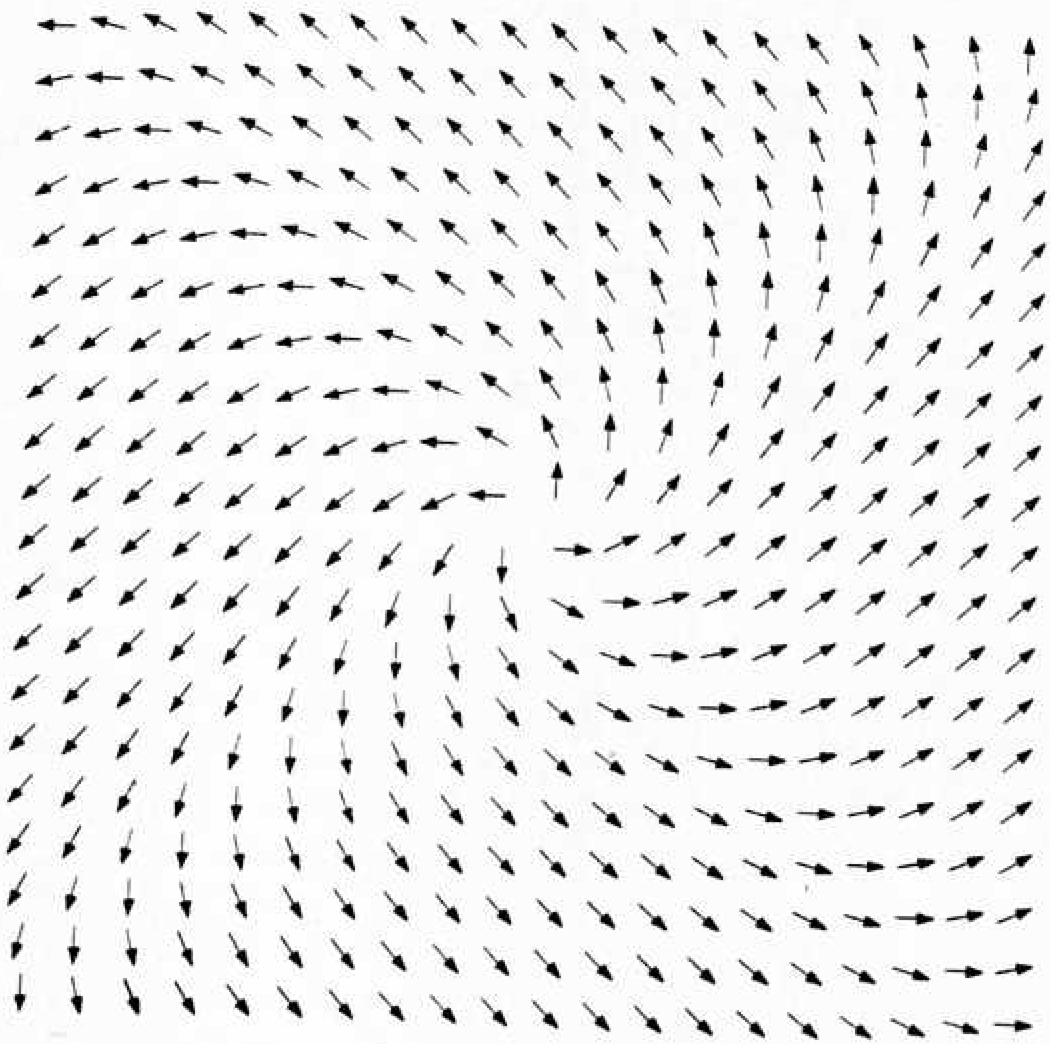

fig. 1

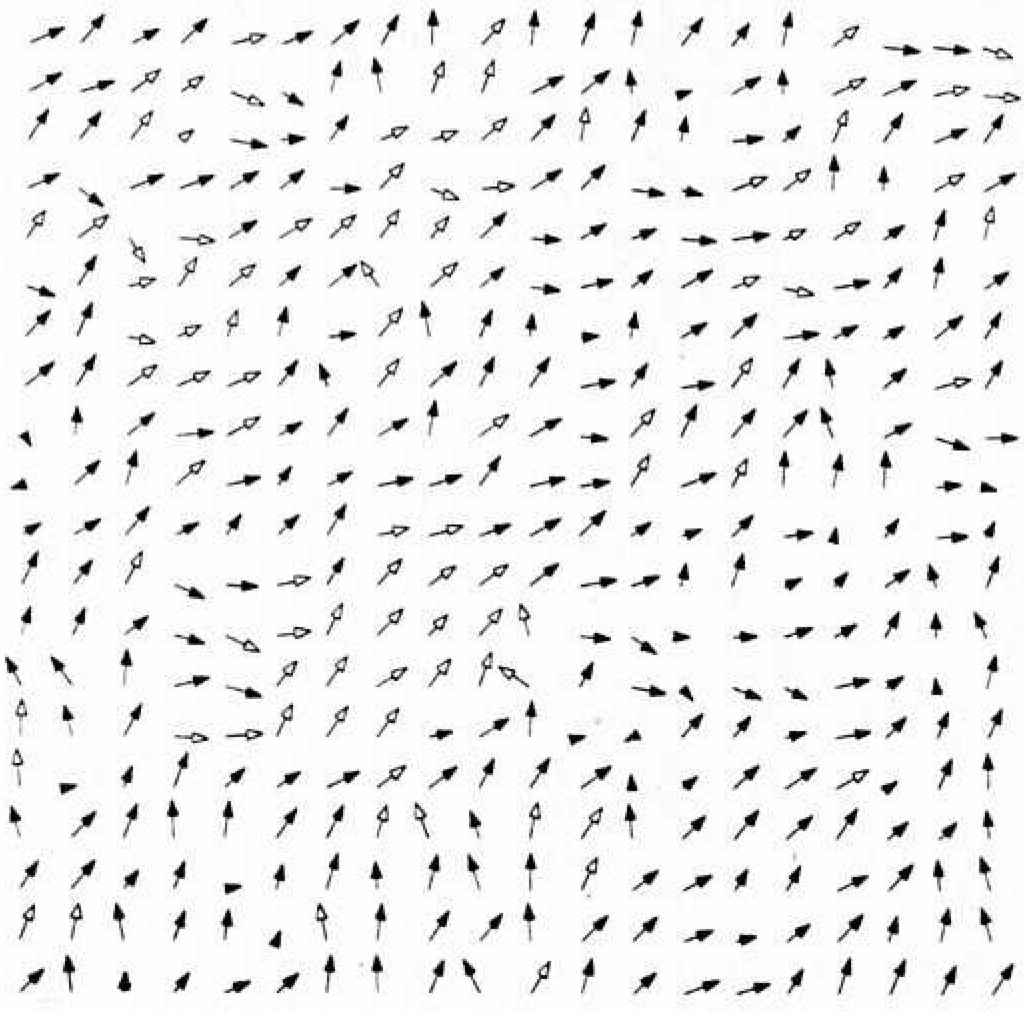

fig. 2a $T = 0.4\,JS^2$

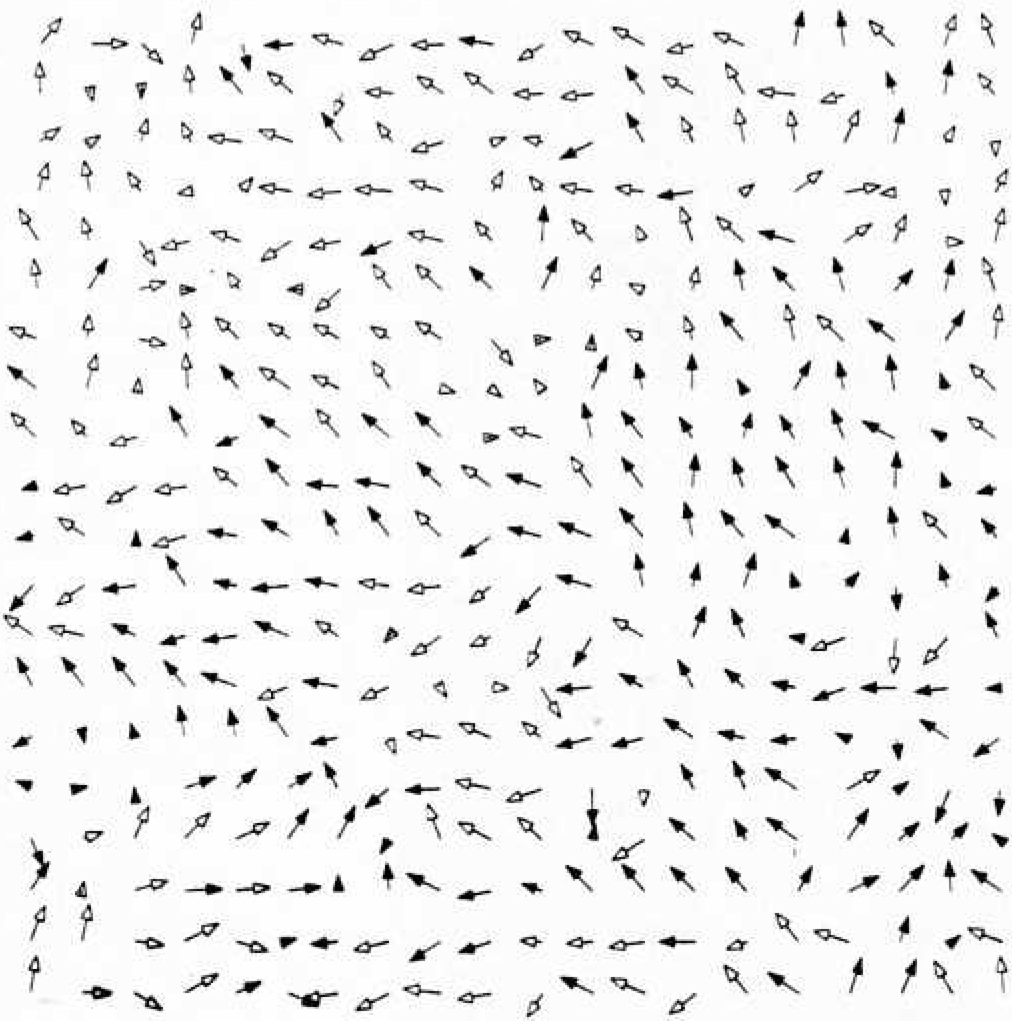

fig. 2b $T = 0.7\,JS^2$

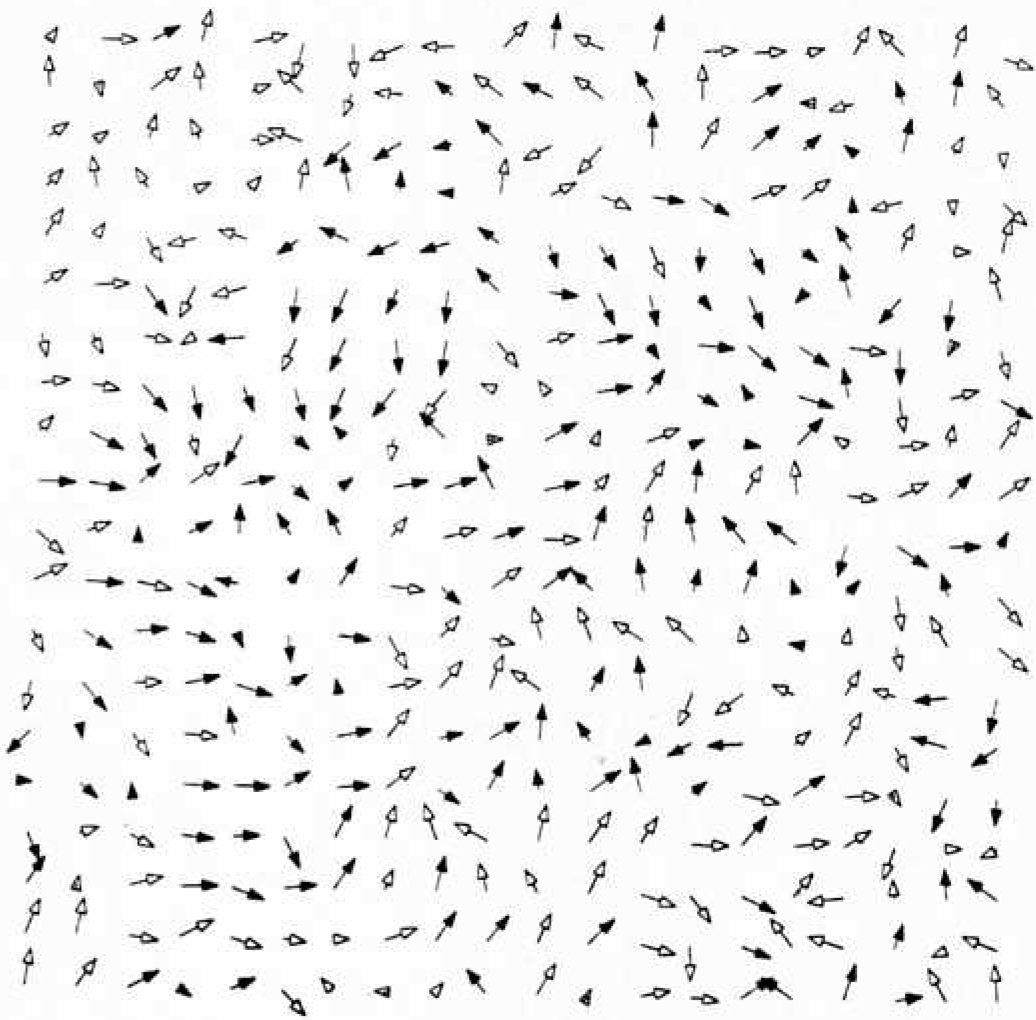

fig 2c $T = 0.9\,JS^2$

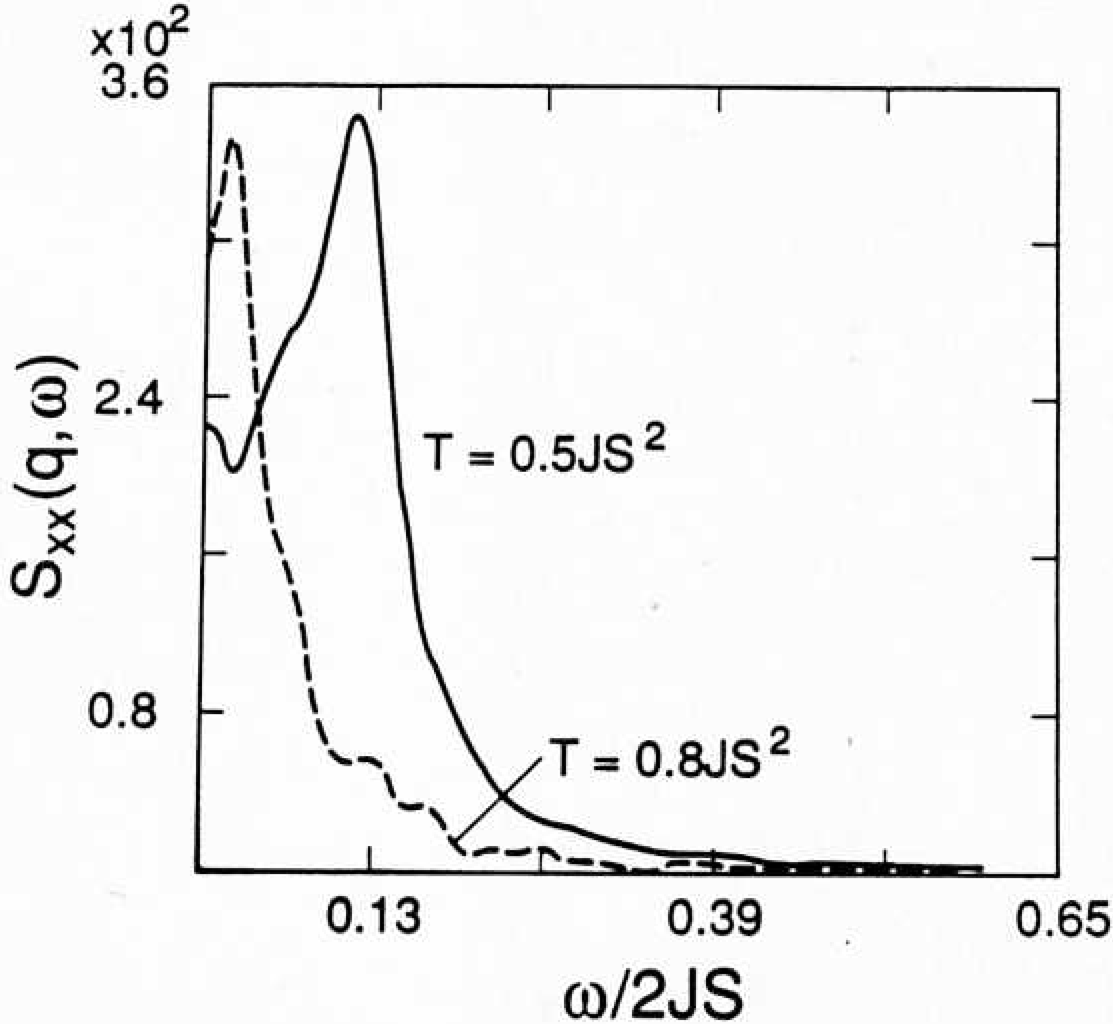

fig. 3a

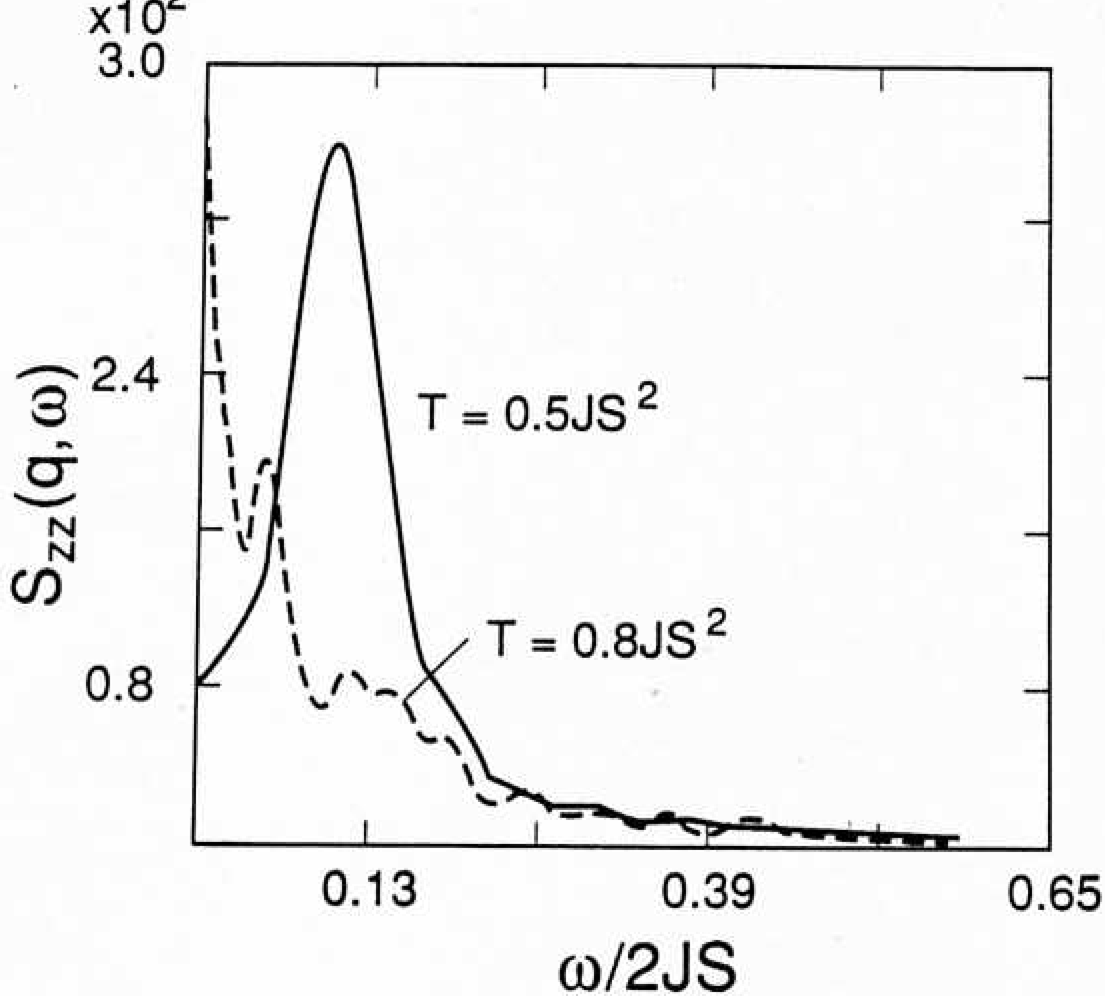

fig 3b

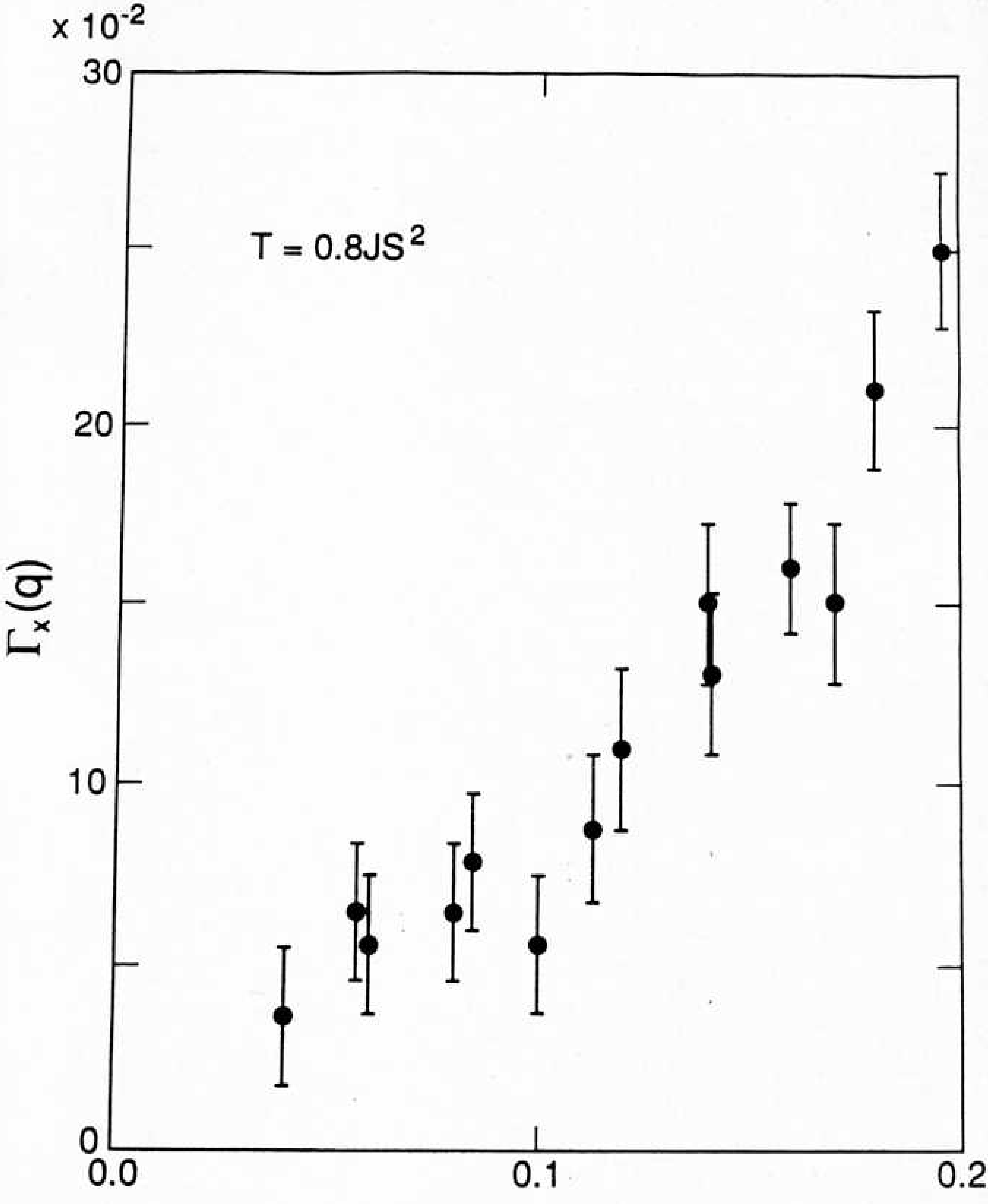

fig 4a

88096602-7.adb

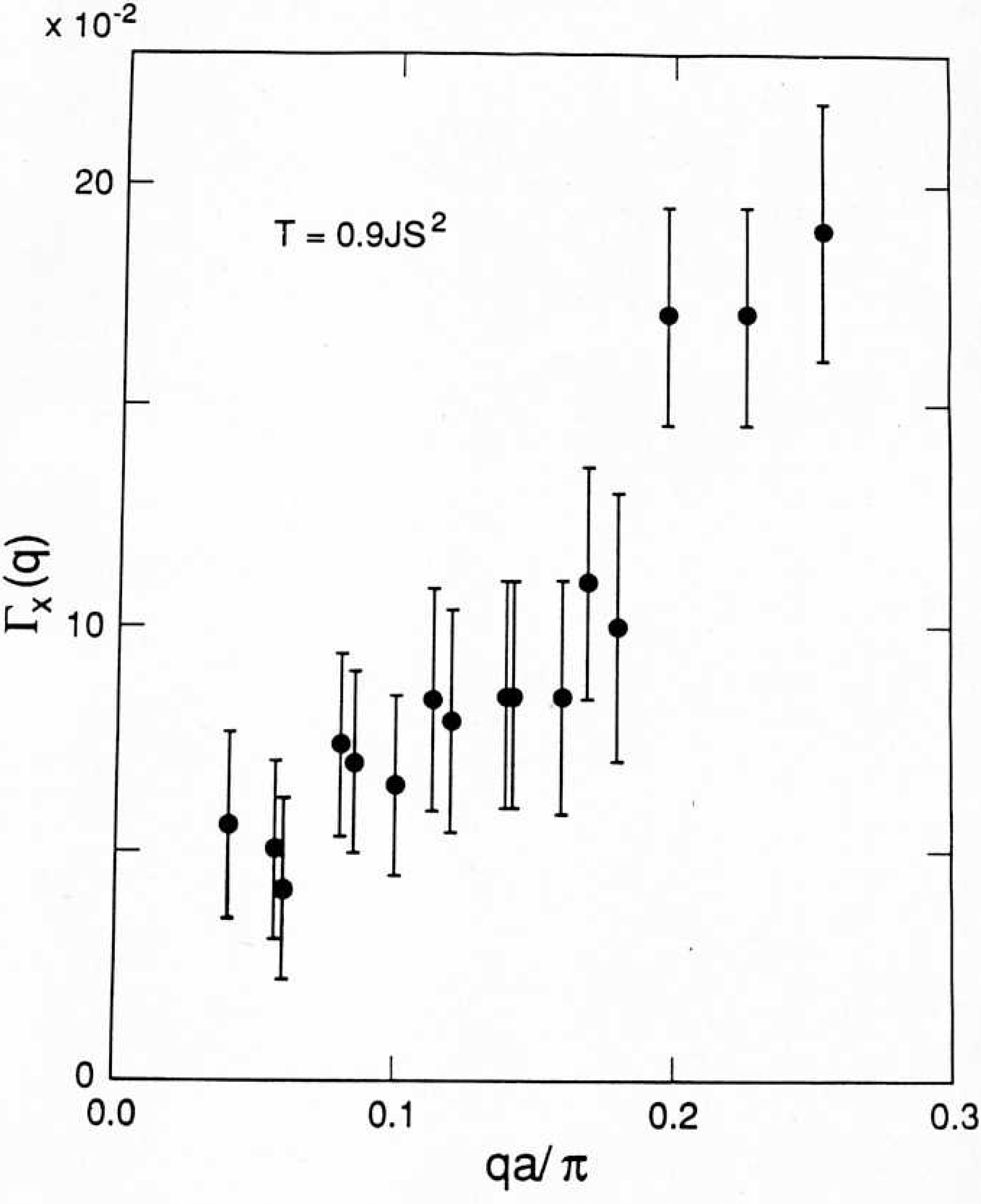

fig 4b

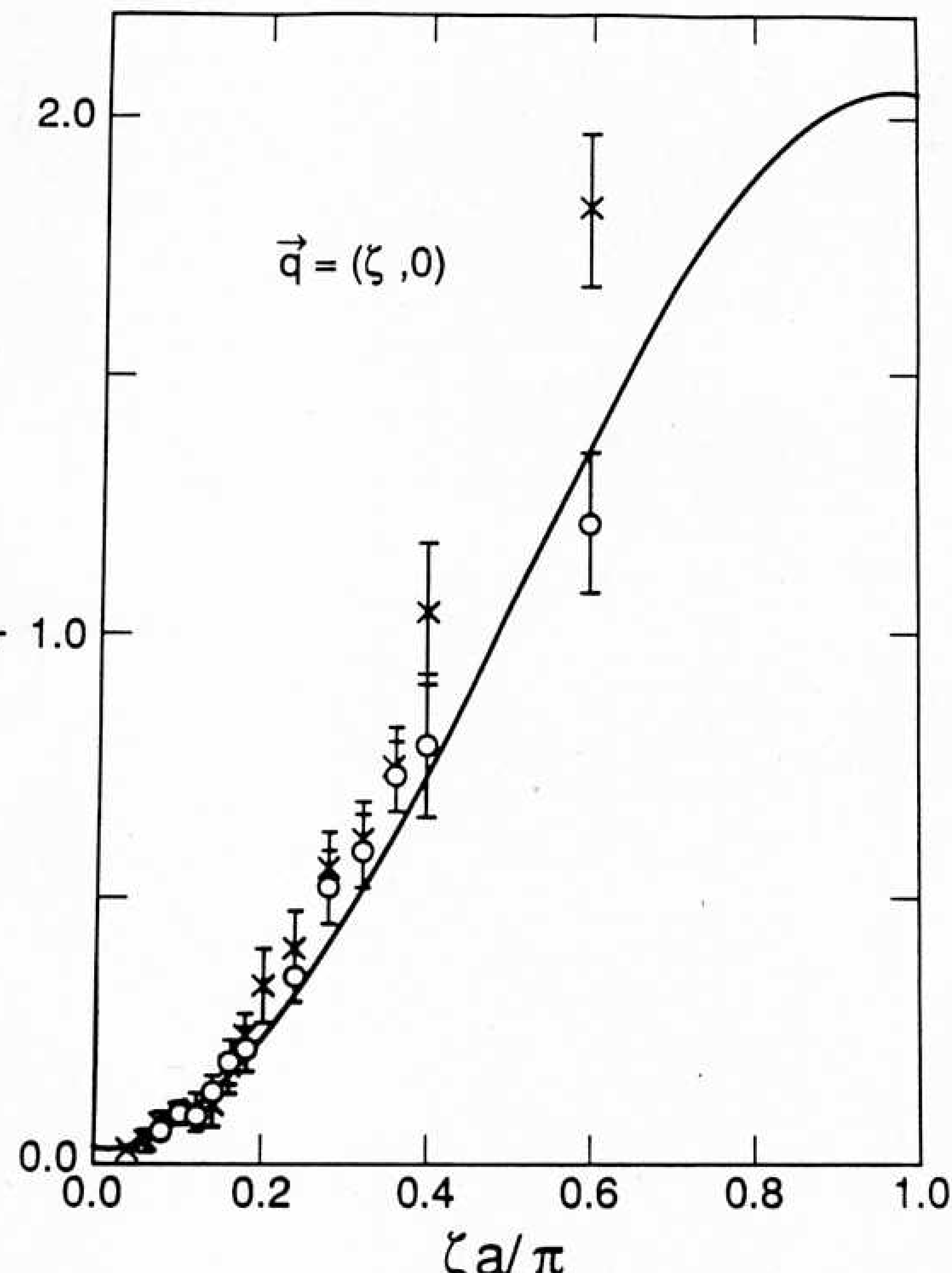

fig. 5a

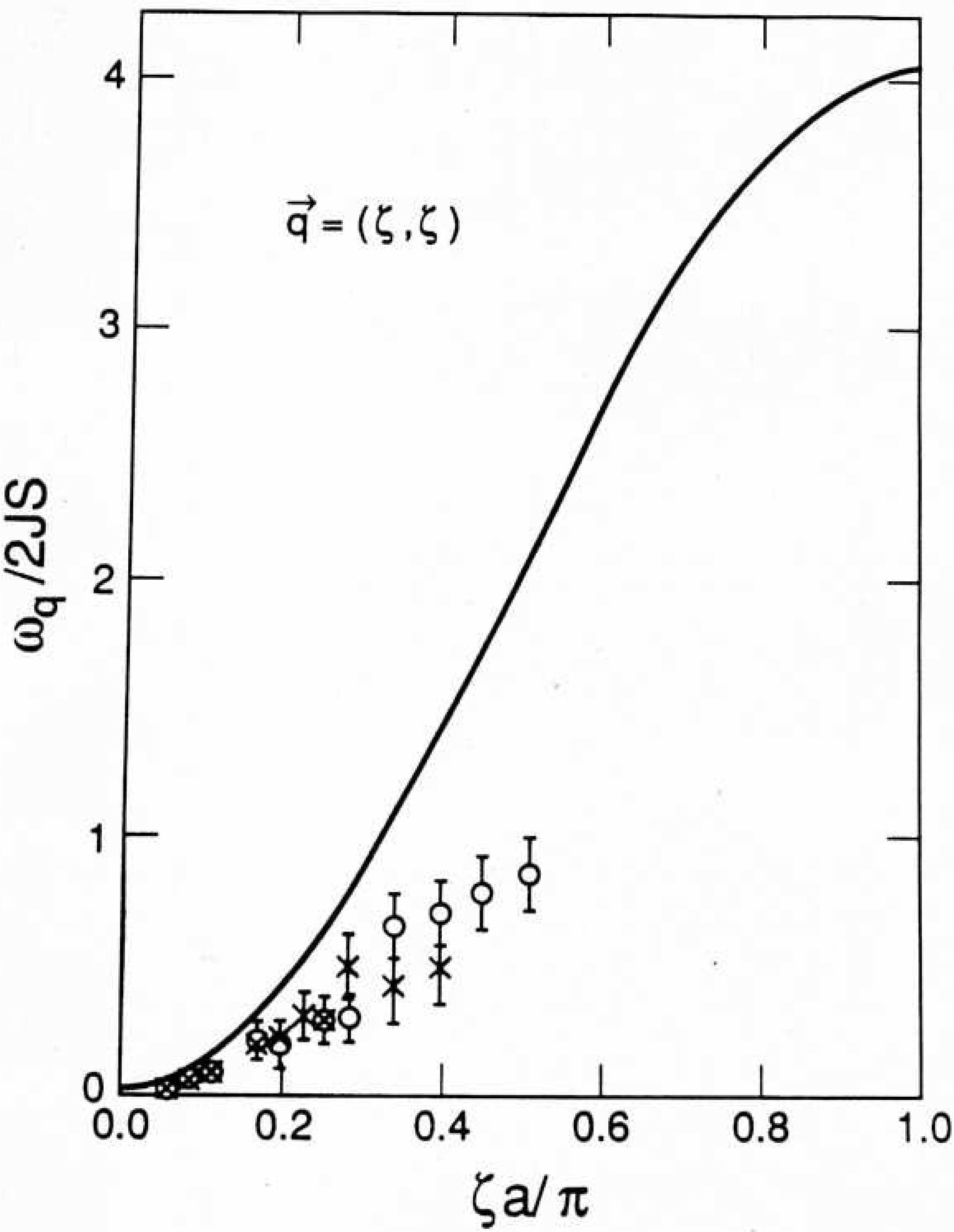

fig. 5b

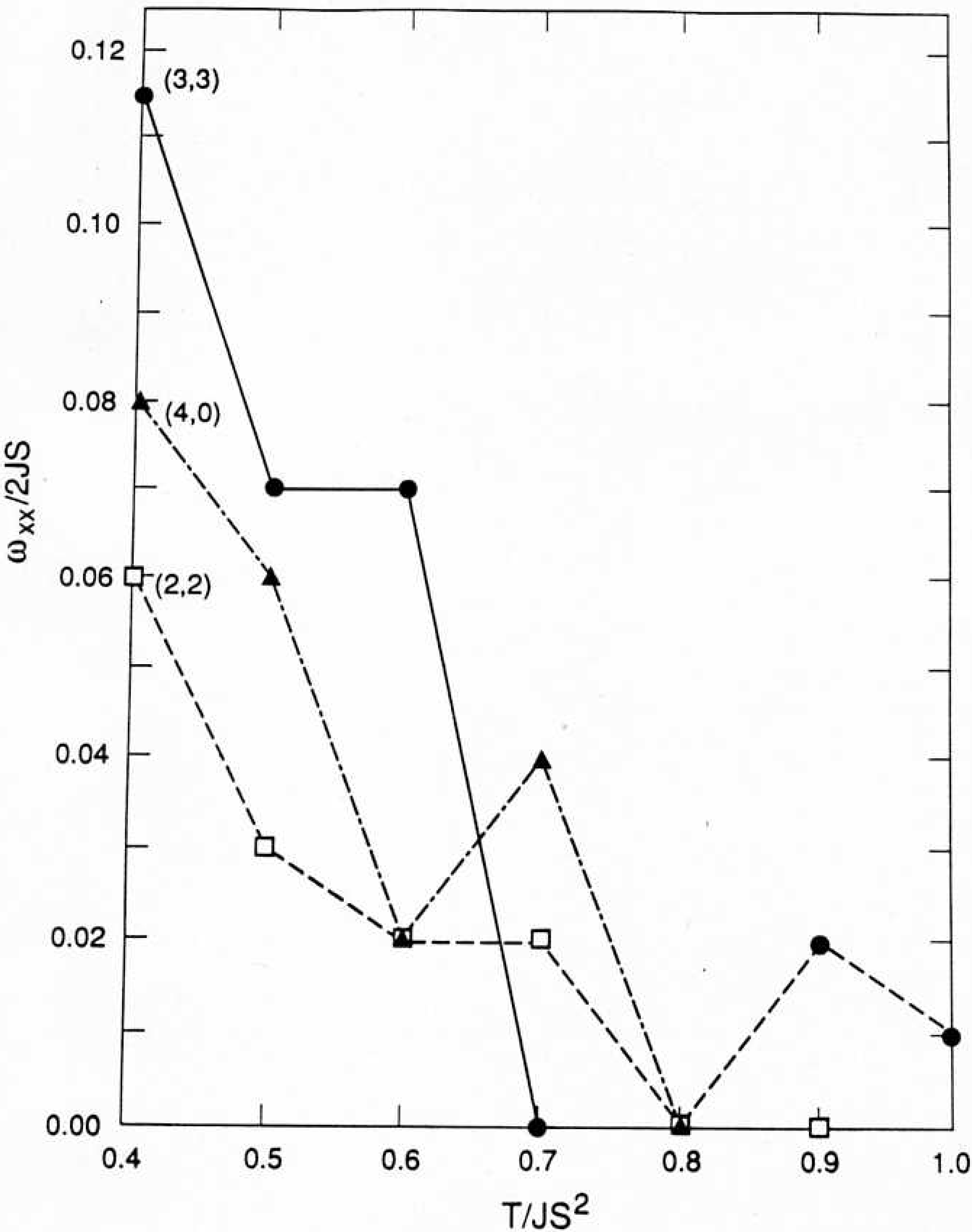

0.12
0.10
0.08
0.06
0.04
0.02
0.00
(3,3)
(4,0)
(2,2)
ω_xx/2JS
0.4
0.5
0.6
0.7
0.8
0.9
1.0
T/JS²

fig 6a

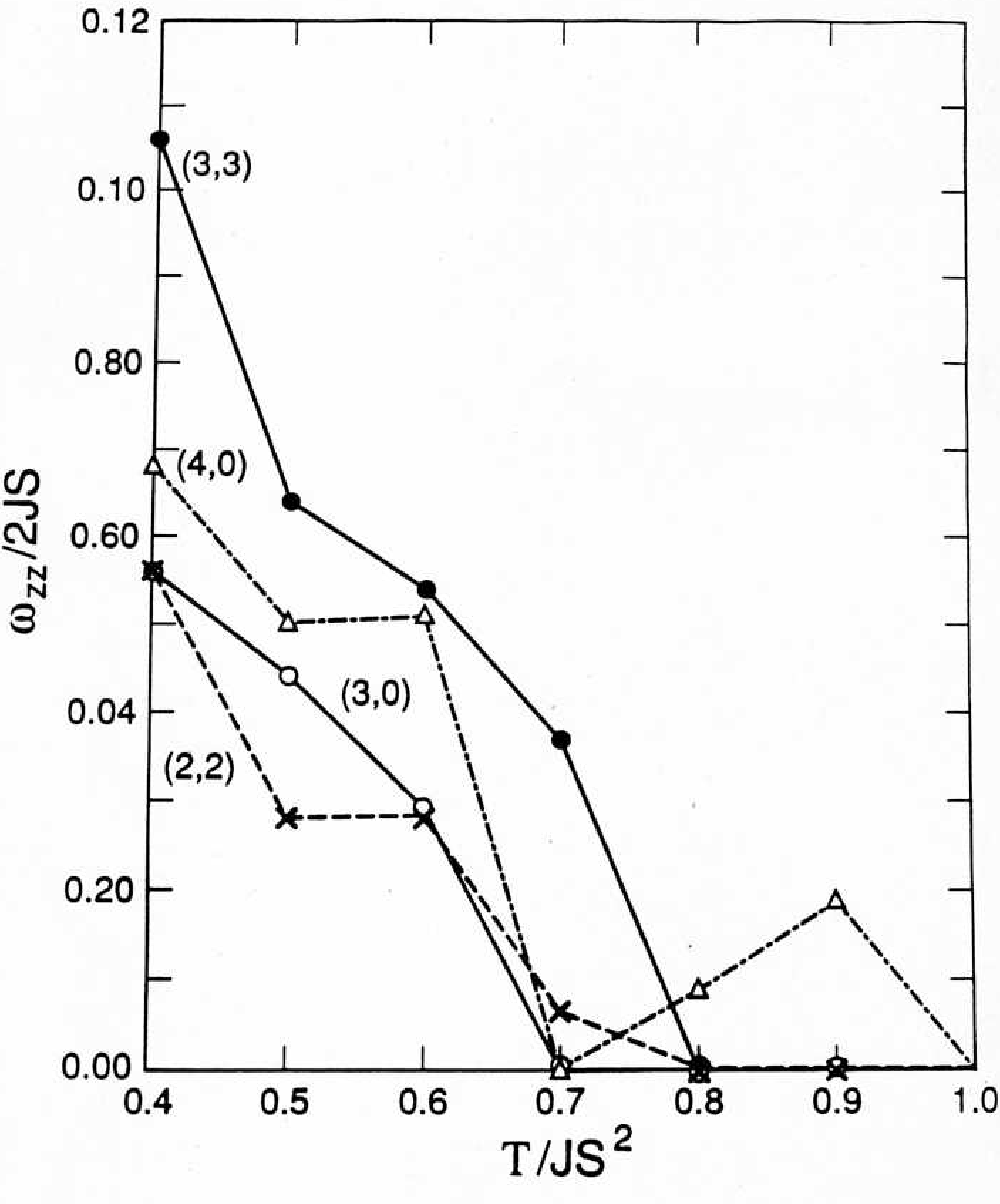
0.12
0.10
0.80
0.60
0.04
0.20
0.00
0.4
0.5
0.6
0.7
0.8
0.9
1.0
$\omega_{zz}/2JS$
T/JS^2
(3,3)
(4,0)
(3,0)
(2,2)

fig. 6b

86096602-8.adb

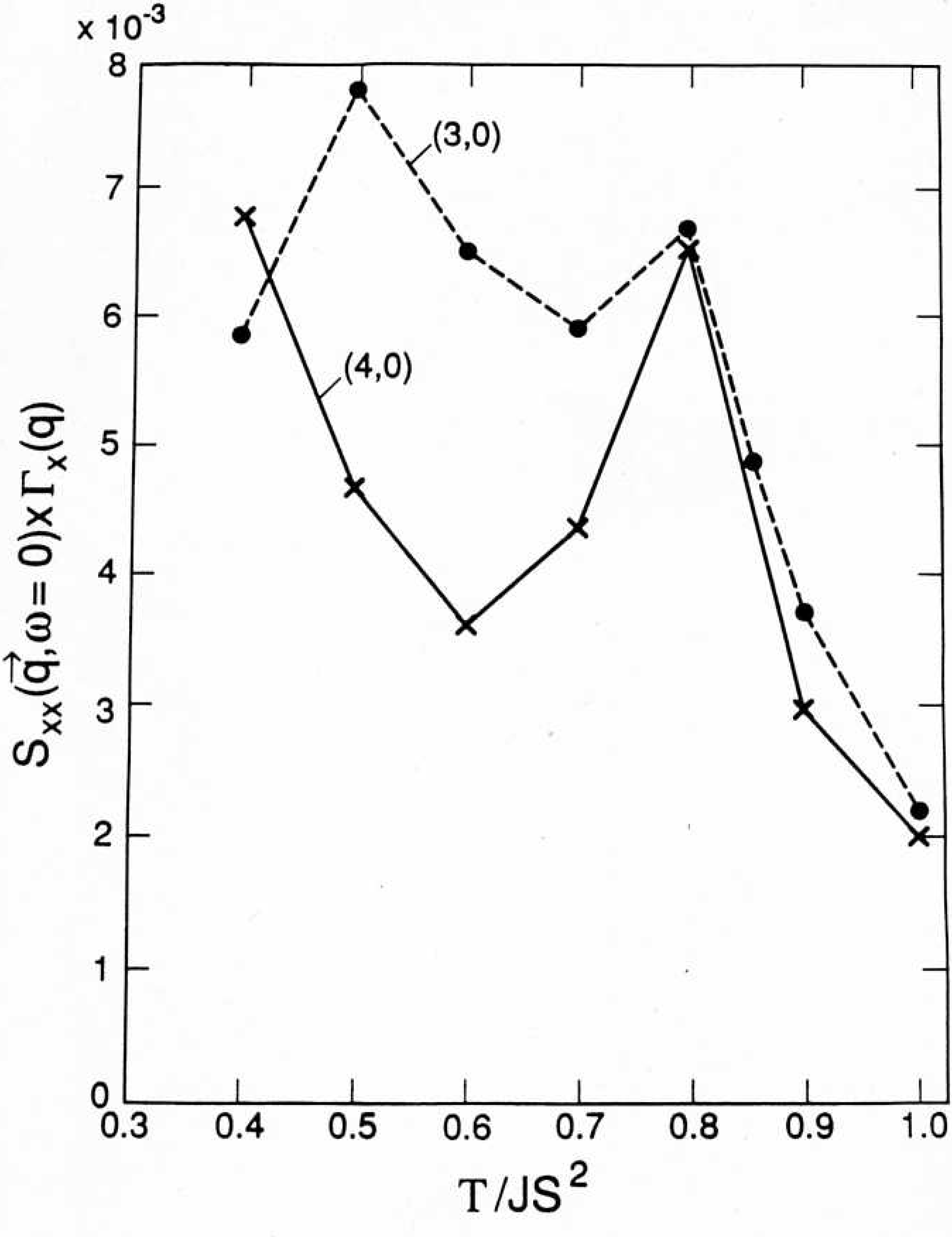

Fig 7a

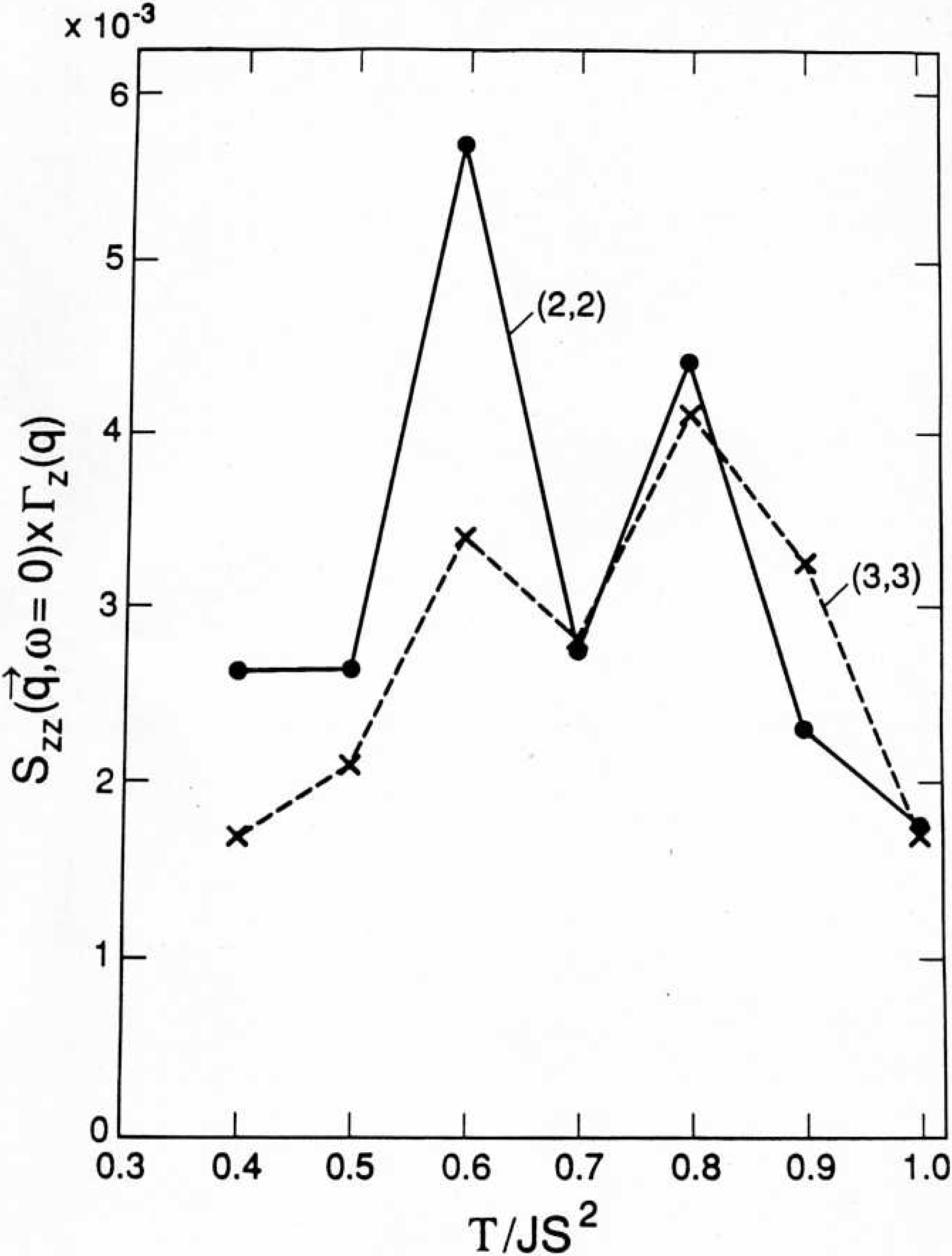

Figure 7b